Available online at www.sciencedirect.com
SCIENCE DIRECT
Materials Chemistry and Physics 96 (2006) 343–348
MATERIALS CHEMISTRY AND PHYSICS
www.elsevier.com/locate/matchemphys

Oxidation of 1018 carbon steel in borate medium by in situ EC-STM: Surface morphology of the oxidized ferrite and pearlite phases

R. Cabrera-Sierra [a,b], Nikola Batina [b], Ignacio González [b,*]

[a] *Escuela Superior de Ingeniería Química e Industrias Extractivas (ESIQIE-IPN), Departamento de Metalurgia, UPALM Zacatenco AP 75-874, C.P. 07738, D.F., Mexico*
[b] *Universidad Autónoma Metropolitana-Iztapalapa, Depto. de Química, Área de Electroquímica, Apdo. 55-534, C.P. 09340, México, D.F., Mexico*

Received 17 November 2004; received in revised form 24 June 2005; accepted 19 July 2005

Abstract

Microstructures of low carbon steel are ferrite (Fe-α) and pearlite (alternate mixture of Fe-α and Fe_3C) and each one has its own oxidation mechanism. These two phases were identified using in situ electrochemical scanning tunneling microscopy (EC-STM). Real time images were obtained during the immersion of 1018 carbon steel probes in 0.642 M H_3BO_3 and 0.1 M NaOH, pH 7.8. Two different corrosion mechanisms (oxide characteristics) were identified and correlated with the observed surface changes.

Keywords: EC-STM; Corrosion; Microstructure

1. Introduction

Carbon steel corrosion in the aqueous media is one of very often studied systems because of its impact in the chemical industry. The carbon steel–aqueous media interface has been subject of numerous in situ electrochemical studies and ex situ microscopies and spectroscopies [1–8].

As it is well known, depending on the fabrication process, on the carbon steel surface two different phases: ferrite, Fe-α (iron rich phase), and pearlite (sequential arrangement of ferrite and iron carbide, Fe_3C) [9], can be found. The microstructural characterization and detail phase identification is possible to carry out by using different microscopies [9]. However, corrosion studies, mainly based on use of electrochemical techniques, of a steel interface in an aqueous medium do not consider oxidation mechanism for separate phases. Such studies in general offer information on the oxidation mechanism of the complete interface [1–8].

Our study, presented here is based on the assumption that oxidation mechanism of each phase on the carbon steel surface is different and can be determined using an in situ real time monitoring method by scanning tunneling microscopy (STM). The STM technique, so far, has been broadly used to identify atomic arrangements of corrosion products on monocrystalline materials (well-defined surface of Cr, Fe–Cr, Fe–Cr–Ni, Cu, Ni) [10–14]. In other studies [10–12] spectroscopic techniques, such as XPS, has been used to determine the chemical composition of the corrosion products (oxides). The iron–borate interface has been broadly studied in the literature [15–25], too. In majority studies, it is suggested that iron oxides formed under the potentiostatic control exhibits great reversibility in the oxidation–reduction process. However, there are some discrepancies concerning the chemical composition of corrosion products and the formation–reduction reversibility of these compounds [22,24].

More recently, in situ characterization of the polycrystalline iron corrosion products in borate solutions (at different pH's) have been carried out using electrochemical scanning tunneling microscopy (EC-STM), electrochemical atomic force microscopy (EC-AFM) and XPS [17,19,22,24].

* Corresponding author. Tel.: 52 55 58044671; fax: +52 55 58044666.
E-mail addresses: rcabreras@ipn.mx (R. Cabrera-Sierra), igm@xanum.uam.mx (I. González).

0254-0584/$ – see front matter © 2005 Elsevier B.V. All rights reserved.
doi:10.1016/j.matchemphys.2005.07.049

Consequently, it has been established that film formation on the iron surface in borate medium can be described by two-layer model, which consists of an internal layer (near the substrate) corresponding to magnetite (Fe_3O_4) and another, external, identified as maghemite (γ-Fe_2O_3) [15,18,20,23,25]. The relationship between these two oxides formed by using potential regime (magnetite/maghemite) decreases as the oxidation potential becomes more positive [18,20]. Thus, the maghemite formation is greater at higher oxidation potentials.

In our study here, based on use of EC-STM for 1018 carbon steel characterization, these previous findings were taking into account, too. As well we presume that oxidation behavior and oxide characteristics of each phase and oxide layer will be different and distinguished by EC-STM. One should note that steel phase with higher proportion of iron [9] could show higher reactivity toward the oxidation process. Another important assumption in our study is based on possibility to identified different phases on the steel surface, and monitoring the oxide layer development. In final, it leads to better understanding of the corrosion mechanism of ferrite and pearlite, as well as steel surface in general. Our results clearly show that EC-STM allows identification of both phases on the 1018 carbon steel–borate interface and could distinguish different steps and mechanisms during the oxide layer formation.

2. Experimental

2.1. Preparation of the electrolytic medium

The electrolyte, a borate buffer solution (pH 7.8) was prepared from 0.642 M H_3BO_3 and 0.1 M NaOH. Ultra pure water (Millipore, 18.2 MΩ cm) and Merck analytic reagents were used.

2.2. Sample preparation.

The working electrode was 1018 carbon steel with a surface area of 0.33 cm^2. This material has a typical composition of 0.14–0.20% C, 0.60–0.9% Mn, 0.035% maximum S, 0.030% maximum P and the rest is composed of Fe [9]. 1018 Carbon steel discs were polished with silicon carbide emery paper (grade 400), emery paper (grade 600) and finished with 0.3 μm aluminum oxide powder to give a mirror appearance. Between polishing, samples were washed with pure water, and finally clean by ultrasonic washing during 5 min with acetone. More details are available in our previously published papers [26,27].

2.3. Equipment

Electrochemical scanning tunneling microscopy studies were performed using a STM microscope from Molecular Imaging with a Picostat (bipotentiostat) adapted to an electrochemical cell. A STM electrochemical cell was made of Teflon with exposed sample area of 0.33 cm^2. Platinum and copper oxide/copper wires were used as a counter and pseudoreference electrodes, respectively. The pseudoreference electrode (Cu_2O [13]), prepared in our laboratory, showed a great stability in the borate medium with a constant potential of 0.140 V versus NHE. All the potentials presented in this work are quoted with respect to the normal hydrogen electrode (NHE). STM tips were prepared by electrochemical etching of tungsten wire in a 6N NaOH solution and covered with a nail polish [28]. The usual imaging conditions were a bias potential of −0.18 V and a set point current of 2–3 nA. EC-STM images were recorded in the constant current mode and at the open circuit potential (OCP). Images were recorded and presented as a function of time. Every study was repeated several times always on a freshly prepared electrode.

3. Results and discussion

3.1. Surface characterization of a carbon steel surface in borate medium using in situ EC-STM at the open circuit potential

It is important to indicate that the experimental methodology proposed in this work for surface characterization of 1018 carbon steel in borate medium using in situ EC-STM technique is different from that reported in previous works [17,19,22,24,29]. In these works, the surface characterization was carried out after cleaning the sample surface from the corrosion products (native oxide), through an imposed cathodic potential. In order to differentiate the reactivity of distinct microstructures on the basis of oxidation mechanism of each steel phase, our work focuses on monitoring the evolution of corrosion process of the steel–aqueous solution interface from the immersion time zero (to capture the early stages of the corrosion process, at OCP conditions).

As a preliminary step, the 1018 carbon steel surface immersed in the borate electrolyte, was imaged by EC-STM, at the open circuit potential, thus from the beginning of immersion. However, the OCP was changed gradually during the first 2 min (these measurements were made on a standard electrochemical cell, out of EC-STM), from −0.030 to −0.125 V versus NHE. During this time it was not possible to obtain a high quality images. Afterwards, the OCP was maintained constant with the immersion time allowing to apply a constant E_{bias} during image recording by STM in situ (E_{bias} = −0.180 V). The optimum E_{bias} was obtained by changing the tip potential, and maintaining the sample potential constant at −0.125 V versus NHE. Before continuing our experiments, we demonstrated that different bias potentials (E_{bias}), applied between the tip and the sample, do not alter corrosion process on the sample surface.

After a systematic analysis of the large part of the electrode surface, at different immersion times, we identified only two types of structures and related corrosion processes. Figs. 1 and 4 show EC-STM images (OCP) obtained in situ during immersion of a carbon steel sample in the borate medium pH 7.8, related to the observed structures.

3.2. Continuous change of a carbon steel surface during immersion time in the borate solution, monitored by EC-STM—ferrite microstructure

Fig. 1 shows a series of typical in situ EC-STM images observed during continuous monitoring of surface changes of 1018 carbon steel after different immersion time (23, 36 and 56 min) in the borate medium, at pH 7.8, respectively, Fig. 1a–c. In all three images a granular oxide growth is visible, with clear indication of the coalescence of the oxide nodules, i.e. two times during 13 min (Fig. 1a versus b). After 56 min (Fig. 1c), surface morphology does not change significantly any more. It seems that oxidation process reached a steady state or it is related to development of different type of oxide. See above mentioned possibilities and literature findings.

Fig. 2 presents a cross-section analysis corresponding to surfaces in Fig. 1a (23 min) and Fig. 1c (56 min). This surface analysis was carried out using image treatment software that fixes a minimum reference point (1) and a maximum point (2) on the reference line (see white dotted lines in Fig. 1a and c). This simple analysis shown in Fig. 2 illustrates a general trend of the increase of the surface corrugation as a function of the immersion time. It is expected results of the oxide nodule coalescence process. At lower immersion times (Figs. 1a and 2a), the individual grains posses size in the range between 0.43 and 1 μm. At longer time of immersion, they coalescence of oxide into larger nodules 1.5–2 μm (Figs. 1c and 2b). However, one could also observed very fine features in the size range between 0.2 and 0.41 μm, at this large nodules.

Variations for minimum and maximum height (surface corrugation) as a function of the immersion time are shown in Fig. 3a. It is constant due to the early stage of the oxide growth between 13 and 40 min. Than at 56 min corrugation becomes much larger. In order to have a better idea of the surface properties, we also evaluate the surface roughness (rms) from the obtained images. Fig. 3b clearly shows gradually and continuous (almost linear function) increase of the surface roughness during progress of the surface oxidation. The observed behavior we intent to associate to oxidation of the iron-rich phase of carbon steel (ferrite), due to reasons, which we will discussed further on.

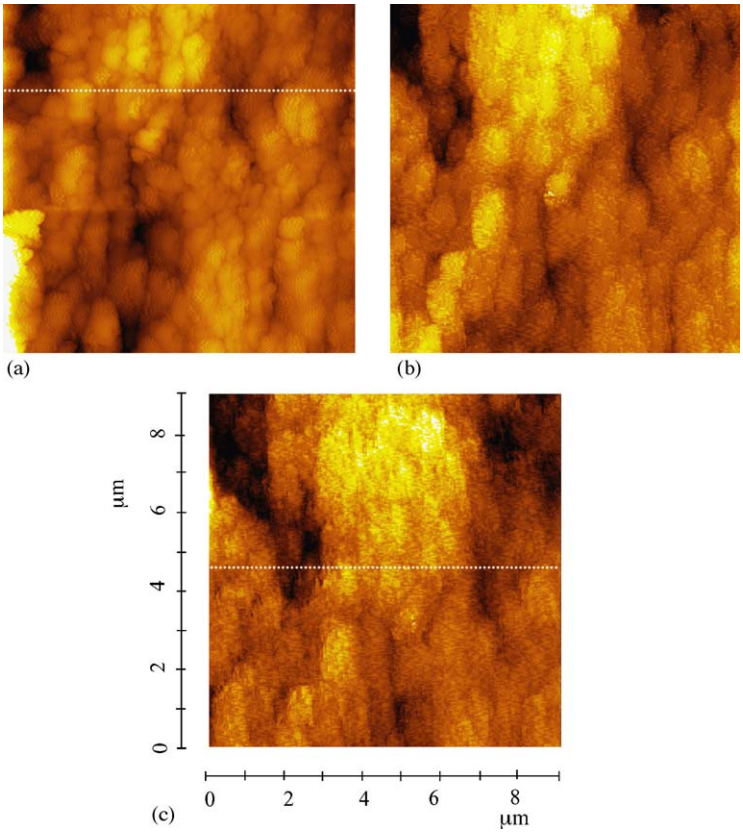

Fig. 1. In situ EC-STM images of 1018 carbon steel immersed in 0.642 M H_3BO_3 and 0.1 M NaOH, pH 7.8, after different immersion times: (a) 23 min, (b) 36 min and (c) 56 min (ferrite phase). The images were recorded at open circuit potential. *Z* scale: 0–250 Å.

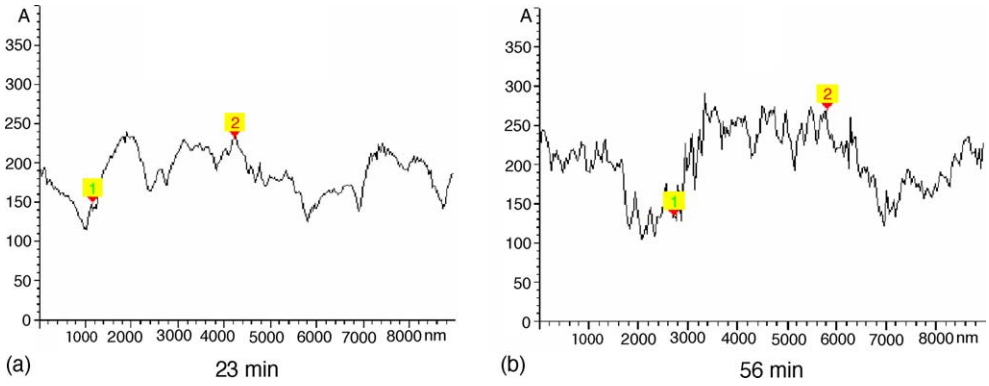

Fig. 2. Cross-section analysis for images (ferrite) obtained on 1018 carbon steel in 0.642 M H_3BO_3 and 0.1 M NaOH, pH 7.8, after two different immersion times: (a) 23 min and (b) 56 min. Marker 1 and 2 represent the minimum and maximum points, respectively, in the selected reference lines shown in Fig. 1.The cross-section analysis was performed on the white dotted lines marked in the figure.

3.3. Continuous change of a carbon steel surface during immersion time in the borate solution, monitored by ECSTM—pearlite microstructure

Fig. 4 shows the second typical surface obtained for 1018 carbon steel immersed in 0.642 M H_3BO_3 and 0.1 M NaOH, pH 7.8 at the OCP potential. Images were collected during the period of time between 11.5 and 84 min. Images are of the high quality, and imaging was possible from the beginning of the experiment. No noticeable changes were observed during the EC-STM image recording during first 11.5 min of immersion (Fig. 4a), which indicates on slow oxidation process and associated with the lower reactivity towards corrosion. Definitively it can be related to the difference in the surface composition-microstructure, which is confirmed in further analysis.

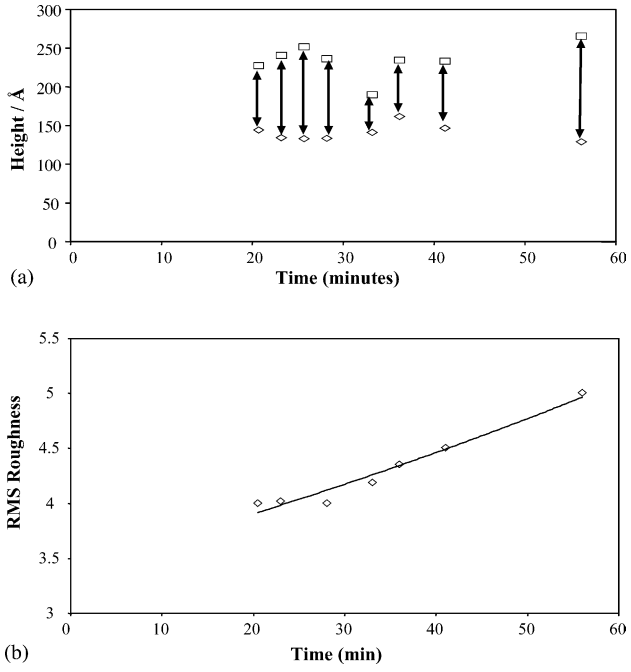

Fig. 3. (a) Height variations of minimum (◊) and maximum (□) points, selected from the cross-section analysis and (b) roughness analysis (rms), during the immersion time of 1018 carbon steel in 0.642 M H_3BO_3 and 0.1 M NaOH, pH 7.8 (ferrite).

Images in Fig. 4 revealed a very specific microstructure of the steel surface with clear linear features (ridges) running along the electrode surface. At the beginning, we tended to associate these lines with the sample polishing treatment. However, this hypothesis was discarded because the observed ridges are significantly thinner (100 nm or 0.1 μm) than polishing particles used in the abrasive paper during sample preparation. Furthermore, this specific structure was observed only at the same part of the surface, not overall, what one expect to be result of the sample preparation. In addition, we also carefully review the literature reporting AFM images of the polished metal and oxide surfaces. In all reports, see, for example, Fig. 11 in Sanz and co-worker [24], polishing lines running over freshly polished surface, always in different directions as a result of polishing treatment. Lines produced on the metal surface by polishing procedure, look like channels (depressions) (dark-colored lower part in the AFM topography images) [30,31].

Therefore, we conclude that regularly distributed aligned ridges, observed in our Fig. 4a, do not result from the sample polishing treatment. Furthermore, as very strong argument, we found that observed STM features are closely related to the microstructure of the carbon steel phase known as pearlite [32,33]. Namely, the surface topography in our STM images is very similar to that seen in scanning electron microscopy (SEM) and reported in previous works [32,33]. Indeed, the distance between the observed line features in SEM (0.095 μm) and STM images (0.1 μm) is the same. To our knowledge, we are the first reporting the pearlite structure obtained by EC-STM images. In addition, we are also able to measure depth height of the observed ridges: 8–10 nm. Note that this microstructure is very different from that reported above. These two distinct microstructures were observed for all samples, and to us should be related to two known phases of the carbon steel sample: pearlite and ferrite.

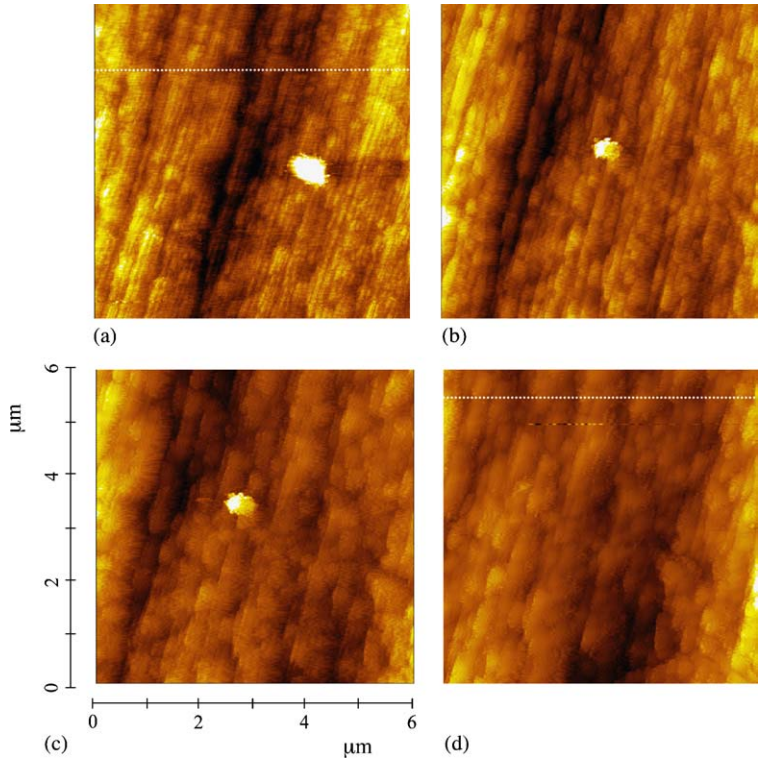

Fig. 4. In situ EC-STM images of 1018 carbon steel immersed in 0.642 M H_3BO_3 and 0.1 M NaOH, pH 7.8, after different immersion times: (a) 11.5 min, (b) 35 min, (c) 47 min and (d) 84 min (pearlite phase). The images were recorded at open circuit potential. *Z* scale: 0–275 Å.

At longer immersion time, i.e. 35 min (Fig. 4b), granular growth of the corrosion layer, was noticed. The width of line features observed on the steel surface increases by time. However, it is clear that oxide growth proceeds in the preferential direction, following the original ridge arrangement. At the same time, the coalescence of initial grains (grain size range: 0.18–0.29 μm) and the formation of bigger ones (grain size range: 0.29–0.58 μm) are observed. After 47 min (Fig. 4c), this phenomenon is even more obvious. Fig. 4d shows the surface after 84 min of immersion. A mild increase in the granular size (grain size range: 0.48–1.04 μm), of corrosion products with regard to Fig. 4c, is noticed. This could be sign that oxidation process had reached a stationary state. There is a relevant aspect in this image concerning the periodic arrangement (row line feature) that persists even at increased times of immersion and material oxidation.

In order to quantitatively evaluate the observed process, a cross-section analysis for the images recorded after different immersion times is made using a reference line and procedure as described above. Fig. 5 shows the cross-section analysis for images recorded after 11.5 and 84 min. Reference line and minimum and maximum points were indicated. Fig. 5a (11.5 min) shows very rough surface. In contrast, after 84 min (Fig. 5b) surface corrugation is significantly

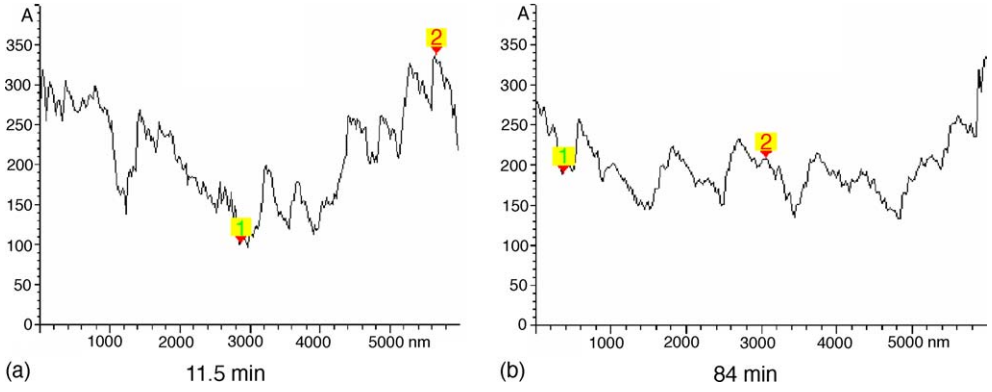

Fig. 5. Cross-section analysis for images (pearlite) obtained on 1018 carbon steel in 0.642 M H_3BO_3 and 0.1 M NaOH, pH 7.8, after two different immersion times: (a) 11.5 min and (b) 84 min. Marker 1 and 2 represent the minimum and maximum points, respectively, in the selected reference lines shown in Fig. 1.The cross-section analysis was performed on the white dotted lines marked in the figure.

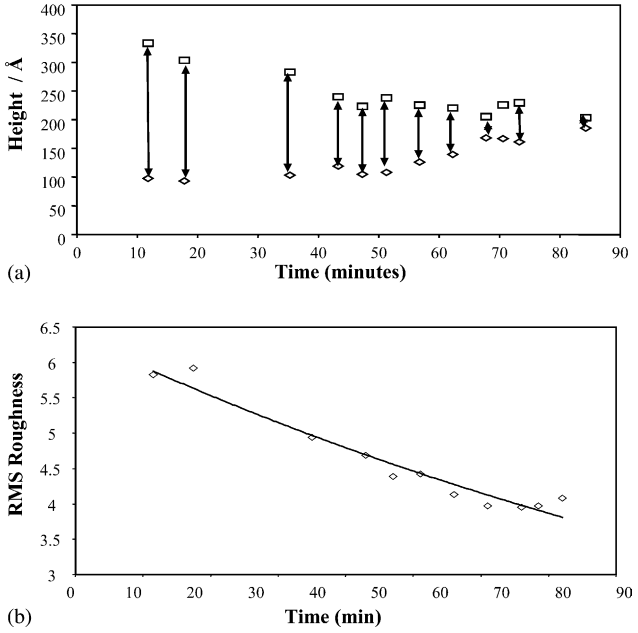

Fig. 6. (a) Height variations of minimum (◊) and maximum (□) points, selected from the cross-section analysis and (b) roughness analysis (rms), during the immersion time of 1018 carbon steel in 0.642 M H_3BO_3 and 0.1 M NaOH, pH 7.8 (pearlite).

diminished. Concerning the height variations relative to the minimum and maximum points, Fig. 6a shows how this surface achieved some kind of a stationary state with low corrugation, after 84 min. Along the same conclusion are results of the roughness (rms) analysis (Fig. 6b), which show decrease of the surface roughness by progress of the immersion time. For the rms and the surface corrugation analysis the same images (Fig. 4) were used. Although from the obtained data it is not possible to understand the mechanism of the observed phenomena of the surface flatness, we tend to believe that it is results of two competitive process, growth and dissolution of the iron oxide layers. However, one also could not exclude that the observed phenomena is results of the change in the oxide growth mechanism, too.

4. Conclusions

Following our idea based on identification of the two different steel structures with different type of oxide, we could conclude that results of our study completely confirmed our hypothesis. Directly (microstructure characterization) and indirectly via different oxidation mechanism, we were able successfully identified different parts of the surface, which can be characterized as, ferrite and pearlite.

Acknowledgments

R. Cabrera-Sierra, is grateful to CONACYT, for his Ph.D. scholarship and COTEPABE-IPN for the academic support. N. Batina is grateful for the support of Instituto Mexicano del Petróleo (IMP, project FIES 98-100-I) and I. González is grateful for the support of Conacyt.

References

[1] T.A. Ramanarayanan, S.N. Smith, Corrosion 46 (1990) 66.
[2] H. Huang, W.J.D. Shaw, Corrosion 48 (1992) 931.
[3] H. Vedage, T.A. Ramanarayanan, J.D. Munford, S.N. Smith, Corrosion 49 (1993) 114.
[4] H. Shutt, P.R. Rhodes, Corrosion 52 (1996) 947.
[5] Y.F. Cheng, J.L. Luo, Electrochim. Acta 44 (1999) 2947.
[6] Y.F. Cheng, J.L. Luo, Appl. Surf. Sci. 167 (2000) 113.
[7] A. Groysman, N. Erdman, Corrosion 56 (2000) 1266.
[8] D.A. Lopez, S.N. Simison, S.R. de Sánchez, Electrochim. Acta 48 (2003) 845.
[9] in: J.R. Davies (Ed.), Properties and Selection: Iron and Steel, vol. 1, 1978; Materials Characterization, vol. 10, 1986, American Society for Metals (ASM), Ohio, USA.
[10] V. Maurice, W.P. Yang, P. Marcus, J. Electrochem. Soc. 141 (1994) 3016.
[11] V. Maurice, W.P. Yang, P. Marcus, J. Electrochem. Soc. 143 (1996) 1182.
[12] V. Maurice, W.P. Yang, P. Marcus, J. Electrochem. Soc. 145 (1998) 909.
[13] V. Maurice, H.H. Strehblow, P. Marcus, J. Electrochem. Soc. 146 (1999) 524.
[14] D. Zuili, V. Maurice, P. Marcus, J. Electrochem. Soc. 147 (2000) 1393.
[15] M. Nagayama, M. Cohen, J. Electrochem. Soc. 109 (1962) 781.
[16] P.C. Searson, R.M. Latanison, U. Stimming, J. Electrochem. Soc. 135 (1988) 1358.
[17] R.C. Bhardwaj, A. González-Martín, J. O'M. Bockris, J. Electrochem. Soc. 138 (1991) 1901.
[18] A.J. Davenport, M. Sansone, J. Electrochem. Soc. 142 (1995) 725.
[19] M.P. Ryan, R.C. Newman, G.E. Thompson, J. Electrochem. Soc. 142 (1995) L177.
[20] L.J. Oblonsky, A.J. Davenport, M.P. Ryan, H.S. Isaacs, R.C. Newman, J. Electrochem. Soc. 144 (1997) 2398.
[21] M. Büchler, P. Schmuki, H. Döhni, J. Electrochem. Soc. 145 (1998) 378.
[22] J. Li, D.J. Maier, J. Electroanal. Chem. 454 (1998) 53.
[23] S. Elzbieta, D.D. Macdonald, J. Electrochem. Soc. 147 (2000) 4087.
[24] I. Diéz-Pérez, P. Gorostiza, F. Sanz, C. Müller, J. Electrochem. Soc. 148 (2001) B307.
[25] L. Jun, D.D. Macdonald, J. Electrochem. Soc. 148 (2001) B425.
[26] R. Cabrera-Sierra, E. Sosa, M.T. Oropeza, I. González, Electrochim. Acta 47 (2002) 2149.
[27] E. Sosa, R. Cabrera-Sierra, M.T. Oropeza, F. Hernández, N. Casillas, R. Tremont, C. Cabrera, I. González, Electrochim. Acta 48 (2003) 1665.
[28] N. Batina, T. Yamada, K. Itaya, Langmuir 11 (1995) 4568.
[29] O. Khaselev, J.M. Sykes, Electrochim. Acta 42 (1997) 2333.
[30] M. Miranda-Hernández, M. Palomar-Pardavé, N. Batina, I. González, J. Electroanal. Chem. 443 (1998) 81.
[31] M. Miranda-Hernández, I. González, N. Batina, J. Phys. Chem. B 105 (2001) 4214.
[32] D.G. Enos, J.R. Scully, Metall. Mater. Trans. A 33A (2002) 1151.
[33] S.W. Thompson, P.R. Howell, J. Mater. Sci. Lett. 17 (1998) 869.